Erosion of buffer caused by groundwater leakages based on EMS-application

O. Punkkinen[*,1], V.-M. Pulkkanen[2] and M. Olin[2]
[1]B+Tech Oy, Helsinki, Finland; [2]VTT Technical Research Centre of Finland, Espoo, Finland
*Corresponding author: Laulukuja 4, FI-00270, Helsinki, Finland, olli.punkkinen@btech.fi

Abstract: The bentonite barrier is an essential part of a safe spent fuel repository in granitic bedrock. The issue of saturation phase erosion of bentonite, caused by groundwater leakages, was approached theoretically and computationally. We evaluated numerically the total mass of eroded bentonite out of a cylindrical erosion channel corresponding to the case of fixed channel radius and purely suction induced free swelling, i.e. the rate swelling and erosion are equal. We observed that eroded mass loss as a function of time increases in log-log scale linearly in the active part of the erosion process, i.e. after the initial transient regime of high swelling and before the final decay towards stable buffer. The slope of the mass loss vs. time varies, but is always between 0.7 and 1.0.

Keywords: Bentonite, erosion, free swelling, suction, dry density, nuclear waste.

1. Introduction

During the last decades several countries have launched programs to develop technology of using bentonite in spent nuclear fuel repositories. All the important bentonite properties depend critically on bentonite density; therefore, any potential mass loss or redistribution events must be well characterized. One such event or process and therefore also a significant issue in Finnish BENTO-programme is the erosion caused by groundwater inflow in a deposition hole, see Figure 1. It results in channelled flow adjacent to buffer rock interface causing transport of bentonite particles and redistribution of bentonite.

In this study we concentrate on erosion in a preformed cylindrical channel in a deposition hole that is not affected by the other parts of the depository system, such as backfill nor the tunnel. The main objective has been a theoretical description and computational platform to be compared to existing experimental erosion results. This will be used later to evaluate the total mass loss in different alternative scenarios and to support the design of the key system components buffer, backfill and sealing systems.

This article is organized as follows. In Chapter 2 we present the physical processes behind pre-saturation erosion, and formulate the corresponding equations respectively. In Chapter 3 we go through the approximations applied in this work, and the corresponding simplifications in equations. In Chapter 4 we present the numerical results as a solution to the set of equations introduced in Chapters 2 and 3. Finally, Chapter 5 summarizes the main points and conclusions based on the results.

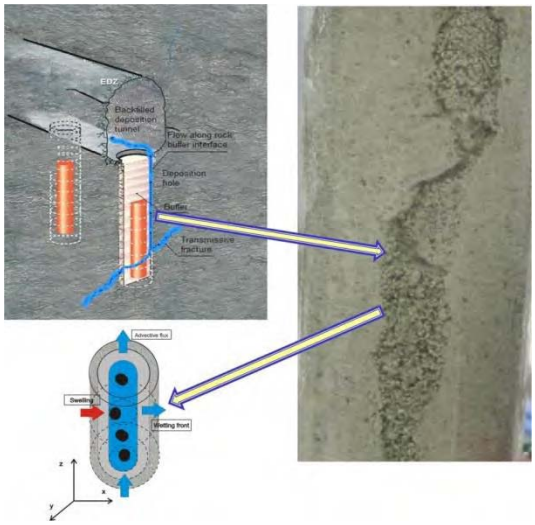

Figure 1. The studied scenario where groundwater inflow into a deposition hole from intersecting leaking fracture results in channeled flow adjacent to buffer rock interface and causes transport of bentonite particles and redistribution of bentonite. The system composes of deposition hole and tunnel .

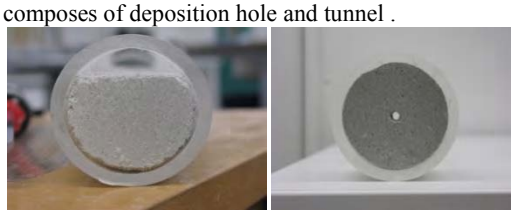

Figure 2. Cross sections of two different flow channel geometries used in tests: Segmental erosion channel (left) and hole erosion set-up (right). The diameter of the cylindrical block is 49.5 mm, and the diameter of pinhole on right hand side is 4mm.

2. Physical and mathematical description of erosion

In pre-erosion process one needs to consider four separate processes in order to fully describe erosion. These are the infiltration of water into a dry clay material, free swelling of partially wet material, detachment of bentonite particles from the water buffer interface, and the dynamics of the detached bentonite particles in eroding flow, see Fig. 8.

On top of these four processes, one also needs to solve the velocity field of water in the erosion channel. Here we resort to an approximation of laminar flow, in which case one can explicitly solve the velocity profile of the eroding liquid in the channel. Given that the volumetric flow rate in typical depository conditions would be fixed to a given value, Q, the solution can be given in terms of the radial coordinate read from the centre of the channel as (Olin 2009, Punkkinen 2010a)

$$\mathbf{v}\ r\ \equiv v\ r\ \mathbf{k} = \frac{Q}{\pi a^2}\left(1-\left[\frac{r}{a}\right]^2\right)\mathbf{k}, \qquad (1)$$

where a is the radius of the cylindrical channel, $\mathbf{k}$ is the unit vector in the direction of gravity, and r is the radial coordinate measured from the centre of the erosion channel, see Fig. 8 (right).

2.1 Wetting, saturation and swelling of buffer bentonite

The channel erosion starts by the wetting of dry bentonite material. It is important to know the velocity of the diffusive wetting front, since this is potentially a decisive factor in determining the width of the bentonite buffer needed to stop the erosion and seal the erosion channel. Typically one uses Richard's equation to predict the saturation profile in porous material as (e.g., Caputo 2009; Punkkinen 2010a)

$$\frac{\partial\theta}{\partial t} = \nabla\left[D\ \theta\ \nabla\theta\right] - S_r\frac{\partial\phi}{\partial t}, \qquad (2)$$

where. The diffusivity of water is related to hydraulic conductivity via $D\ \theta\ = K(\theta)\partial\psi/\partial\theta$, where $K = K\ \theta\ = K\ \phi S_r$ is the unsaturated hydraulic permeability of water in bentonite, and determines the velocity at which the water interface spreads into bentonite. Here is the suction expressed as pressure head in meters, is the total water content defined as volume of water divided by the total volume, and z is the vertical position of cross-sectional surface. In addition, water content is related to saturation and porosity via $\theta = S_r\phi$, where S_r is the saturation, defined as volume of water divided by void volume, and ϕ is porosity, defined as void volume divided by total volume. Furthermore, the dry density of the buffer bentonite ρ_{dry} is related to porosity and to density of the solid bentonite material ρ_s according to

$$\phi = 1-\frac{\rho_{dry}}{\rho_s}, \qquad (3)$$

Usually the unsaturated hydraulic permeability $K(\phi,S)$ is taken to be of product form from the saturated permeability and saturation dependent function as $K\ \phi,S\ = k\ \phi\ f(S)$, where $f(S)$ is usually taken from van Genuchten relations (e.g., Caputo 2008) as

$$K = K_0 k(\phi) S_r^{\frac{1}{2}}\left[1-\left(1-S_r^{\frac{n}{n-1}}\right)^{\frac{n-1}{n}}\right]^2, \qquad (4)$$

Furthermore, the relation between suction and water content, generally known as water retention curve, is typically given by van Genuchten expressions according to

$$S_r \equiv \frac{\theta-\theta_r}{\theta_s-\theta_r} = \left[\frac{1}{1+\ \alpha\varphi\ ^n}\right]^{1-\frac{1}{n}}, \qquad (5)$$

where θ_s is the water content at full saturation, and θ_r is a residual water content at dry material, here assumed to be zero (Villar 2004).

A common way of calculating the solid mass movement is to employ the solid mass balance according to CodeBright (Alonso 1990) as

$$\frac{\partial\rho_{dry}}{\partial t} = \nabla\cdot\left[\rho_{dry}\frac{\mathrm{d}\mathbf{u}}{\mathrm{dt}}\right], \qquad (6)$$

where $\mathbf{u}$ is the deformation field, and is related to the movement of solid buffer material.

The deformation field in bentonite buffer backbone is solved from mechanical equilibrium condition as

$$-\nabla\cdot\boldsymbol{\sigma} = \mathbf{f}, \qquad (7)$$

where $\boldsymbol{\sigma}$ is the stress exerted on bentonite backbone, and $\mathbf{f}$ is the body force exerted on

elastic continuum and the deformation field $\boldsymbol{u}$ is related to strain by $\varepsilon = \frac{1}{2}\left(\nabla \mathbf{u} + \nabla \mathbf{u}^T\right)$. On top of Eq. (7) one needs a constitutive relation between strain and other thermodynamic variables. Under isothermal conditions one typically writes (Alonso 1990) for the elastic part of the strain

$$d\varepsilon = \mathbf{D}^{-1}\left(\boldsymbol{\sigma}, \varphi\right) d\boldsymbol{\sigma} - b\left(\boldsymbol{\sigma}, \varphi\right) \mathbf{I} d\varphi - d\Lambda \frac{\partial G}{\partial \boldsymbol{\sigma}}, \quad (8)$$

where φ is suction, p_0 is atmospheric pressure, $\mathbf{I}$ is an identity matrix, and later one can employ various BBM (Alonso 1990) models for the coefficients (matrixes) $\mathbf{D}, b$ to describe the relation between strain ε and total stress $\boldsymbol{\sigma}$. Typically one chooses $\mathbf{D}$ such that it coincides with the elasticity matrix as

$$\mathbf{D}^{-1} = \frac{1}{E}\begin{bmatrix} 1 & -\nu & 0 \\ \vdots & \ddots & \vdots \\ 0 & \cdots & 2\left(1+\nu\right) \end{bmatrix}, \quad (9)$$

where ν is the Poisson ratio, and E is modulus of elasticity (called Young modulus), and the suction induced bulk modulus is chosen in BBM to follow

$$b = \frac{\kappa_s}{-\varphi + p_0}, \quad (10)$$

where p_0 is the atmospheric pressure.

On top of the nonlinear elastic deformation one generally needs to account for the plastic part of the strain that is described by

$$d\varepsilon^p = d\Lambda \frac{\partial G}{\partial \boldsymbol{\sigma}}, \quad (11)$$

where the plastic potential $G(\boldsymbol{\sigma}, \varphi)$ is given in (Alonso 1990) and $d\Lambda$ is the direction of the plastic deformation. By solving for Eq. (11) one ends up with the more general equation

$$\begin{aligned} &\frac{1}{2}\left(\nabla^2 \mathbf{u} + \nabla\left(\nabla \cdot \mathbf{u}\right)\right) \\ &= -\mathbf{D}^{-1}\mathbf{f} + b\nabla\varphi + \Lambda \frac{\partial G}{\partial \boldsymbol{\sigma}}. \end{aligned} \quad (12)$$

Eq. (12) can be solved with the boundary conditions that the deformation field vanishes at rock buffer interface, and with free deformation at the buffer water interface. The numerical strategy is that one solves for equation (12) in fixed reference coordinate system marked with **r**, and later Eqs. (2) and (6) for water content and dry density are solved in moving coordinate system defined by deformation field as

$$\mathbf{r'} = \mathbf{r} + \mathbf{u(r)}. \quad (13)$$

It should be noticed in a constitutive law Eq. (8), that all the underlying interparticle forces are now buried implicitly into the fitting coefficients $\mathbf{D}, b, G, \Lambda$, and thus they do not show up explicitly for example in the equation of motion for the dry density (6), on the contrary to the formulation by Liu et al. (Liu 2009) and Punkkinen et al. (Punkkinen 2010a).

2.2.Bentonite concentration in erosion channel

Channel evolution can be studied indirectly by assuming a fixed shear stress at the channel walls. A well-known low Reynolds number shear stress ([ ]=Pa) for water reads as (Bonelli 2008, Olin 2009)

$$\tau\left(R\right) = \frac{4\mu(\rho_{dry})Q}{\pi R^3}, \quad (14)$$

where R is the radius of the cylindrical erosion channel. Based on this shear stress one can fit the following production rate of detached particles to experimental data (Bonelli 2008)

$$\sigma\left(R, t\right) = k_{er}\left(\tau - \tau_{cr}\right), \quad (15)$$

where k_{er} is the erosion coefficient ([k_{er}]=s/m) without physical interpretation and τ_c is the critical shear stress needed to remove the bentonite particles from the backbone of the channel.

The mass of the eroded material inside the erosion channel was estimated in the first phase of work using a 2-D axially symmetric erosion model. In this model the mass of eroded material was considered in terms of concentration of eroded solids, c, in a predefined cylindrical erosion channel with as:

$$\begin{aligned} \frac{\partial c}{\partial t} = &\underbrace{\nabla \cdot \left(D_o \nabla c\right)}_{\text{diffusion}} \\ &\underbrace{- \frac{2Q(t)}{\pi R(z,t)^2}\left[1 - \left(\frac{r}{R}\right)^2\right]\frac{\partial c}{\partial z}}_{\text{advection}} \\ &\underbrace{+ 2\frac{\sigma(z,t)}{R(z,t)}}_{\text{detachment}} \underbrace{- \frac{Mg}{\gamma}\frac{\partial c}{\partial z}}_{\text{gravitational settling}} \end{aligned} \quad (16)$$

where the production rate of bentonite particles per surface area is given by Eq. (15), M is the mass on individual bentonite particle, $Q(t)$ is the volumetric flow rate and D_0 is the diffusion

coefficient of bentonite particles in water, being equal to $k_B T/\gamma$, where T is the absolute temperature, k_B is the Boltzmann coefficient and γ is the friction coefficient between individual bentonite particle and the surrounding water, typically assumed to be given by Stoke's law (Liu 2009, Punkkinen 2010a).

3. Suction induced free swelling with fixed channel radius

3.1 Dry density evolution

Based on the preliminary hole erosion tests in a plexi glass column with cylindrical bentonite blocks inside the column, and with prebored hole in the middle of the bentonite cylinders, it was observed that at the end of the test (test time varied between 3 and 8 hours) the radius of the erosion channel was within the error margins the same as the initial radius. This would suggest that particle detachment and swelling of solid material take place in the same pace. This simplifies the equations of motion since now the swelling does not change the total volume of the sample.

Furthermore, we assume that the deformations are nonlinear but elastic, such that plastic part in Eq. (12) can be set to zero. In addition, for coefficient b we assume the typical BBM for (Alonso 1990) given by Eq. (10), where κ_s is the suction induced bulk modulus, related to change in suction, and p_0 is the atmospheric pressure. In the case of unidirectional and radial swelling simply $\nabla(\nabla\cdot\mathbf{u}) \equiv \nabla^2\mathbf{u}$, so that Eqs. (10) and (12) lead to the result

$$\nabla\cdot\mathbf{u}(r,t) = \kappa_s \log\left[\frac{(-\varphi(r',t)+p_0)}{(-\varphi_{0+}p_0)}\right], \quad (17)$$

where r' here refers to the deformed coordinate in accord with Eq. (13). On the other hand, one can formally solve Eq. (6) to obtain an equation of motion for the deformation field as a function of dry density as

$$\nabla\cdot\mathbf{u}(r,t) = \log\left[\rho_{dry}(t{=}0)/\rho_{dry}(r',t)\right]. \quad (18)$$

By combining Eqs. (17) and (18), one arrives at the following result

$$\rho_{dry}\ r',t\ = \rho_{dry}\ r',0\ \left[\frac{-\varphi\ r',t\ +p_0}{-\varphi\ r,0\ +p_0}\right]^{\kappa_s}. \quad (19)$$

Eq. (19) basically neglects the need for solving Eq. (6), and it has an interesting consequence that the dry density at the wet end is fixed as

$$\rho_{dry}\ R,t\ = \rho_{dry}\ r',0\ \left[\frac{p_0}{p_0-\varphi\ r,0}\right]^{\kappa_s}, \quad (20)$$

where R corresponds to the position of the interface between erosion channel and buffer in deformed coordinate system.

Our strategy here is to use Eq. (19) for showing that also the dry density $\rho_{dry}\ r',t$ obeys diffusion type of equation (Punkkinen 2010a). By taking time and spatial derivative of both sides from Eq. (19), leads to the result

$$\frac{\partial\rho_{dry}}{\partial t} = \frac{1}{1+\dfrac{\kappa_s S_r \rho_{dry}}{[p_0-\varphi]\rho_s}\dfrac{\partial\varphi}{\partial\theta}}\frac{\rho_{dry}/\rho_{dry}(r,0)}{p_0-\varphi\ r',t}\frac{\partial\varphi}{\partial\theta} \times\nabla\cdot\left(K_0\frac{p_0-\varphi\ r',t}{\rho_{dry}/\rho_{dry}(r,0)}\nabla\rho_{dry}\right), \quad (21)$$

and where the suction and related (via van Genuchten expressions) saturation degree S_r can be solved independently from Eq. (5). Thus Eq. (22) suggests a diffusion type of equation of motion for the dry density ρ_{dry} in a similar way to which the suction behaves, but with slightly modified coefficients for permeability K and storage factor $\frac{\partial\varphi}{\partial\theta}$.

One can later calculate the mass flux of dry density over the buffer water interface under steady state is equal to the particle detachment concentration, and can be calculated by the gradient of dry density at the interface as

$$\begin{aligned}\sigma\ r' = R,t\ &\equiv D_{dry}\nabla\rho_{dry}\,|_{wet}\\ &\cong -\kappa_s K_0\rho_s\nabla\varphi(R,t)\end{aligned} \quad (22)$$

Thus, in the current model with fixed radius for erosion channel, we set $\tau_c = 0$ in Eq. (18), and take into account the critical force in the level of critical dry density at the buffer water interface. The buffer dry density never drops below this limit, but instead when buffer material reaches the critical density it detaches from the interface. It is important to understand that the detachment

term (22) is an increasing function of the saturated hydraulic conductivity and suction induced bulk modulus. The former speeds up the penetration rate of groundwater into dry buffer, and the latter describes the amount of deformation caused by the suction gradient.

3.2 Concentration and diffusion of detached particles in erosion channel

Under steady state assumption one can furthermore simplify Eq. (16) by including the detachment term (22) into the boundary condition between channel and buffer thus arriving at

$$\frac{\partial c}{\partial t} = \nabla \cdot \left(D_o \nabla c - \left[\frac{Q}{\pi R_0^{\,2}} \left(1 - \left[\frac{r}{a} \right]^2 \right) - \frac{Mg}{\gamma} \right] \frac{\partial c}{\partial z} \right), \quad (23)$$

where we have assumed that the erosion channel is cylindrical as in Figure 1, and that for fixed channel radius the volumetric flow rate becomes constant too. In the following, we have implemented Eqs. (1), (19) and (23) into COMSOL Multiphysics with appropriate boundary conditions. In COMSOL, the water saturation Eq. (1) was solved with *Earth-science module Richard's equation* application mode, and bentonite concentration Eq. (23) with *Multiphysics convection diffusion* equation application mode. To express the relation between suction and saturation we used van Genuchten parameterization (Caputo 2008), see Eq. (5), where $\theta_s = 0.42$ and $\theta_r = 0$ are the full and the initial saturations, $\alpha = 3.2 \cdot 10^{-4}$ m^{-1}/, is a reference inverse pressure, $n = 2.5$ and $m = 1 - 1/n = 0.6$.

If one assumes a laminar channel flow according to Eq. (1) to begin with, and considers a sphere immersed into this parabolic flow, it happens that the sphere feels a lift force called a Magnus effect due to a higher velocity in the center side compared to lower velocity at the wall side of the channel. This force can be approximated by the use of Bernoulli law in radial direction as, and one can derive that the contribution of this force to concentration gradient is (Punkkinen 2010b, Schonberg 1989)

$$D_{radial} \approx \frac{0.56 a_s^{\,2} \rho}{\eta_w} \left(\frac{2Q}{\pi R^2} \right)^2 \approx 4 a_s^{\,2} 10^4. \quad (24)$$

Thus, for clay particles of typical radius $a_s \approx 10^{-6}$ m used in this study, one obtains $D_{radial} \approx 10^{-8}\,\mathrm{m}^2/\mathrm{s}$, which is the value used in most of the simulations.

The viscosity of water is $h = 10^{-3}\,\mathrm{Pa \cdot s}$, the density of water $\rho = 10^3\,\mathrm{kg/m}^3$, the radius of the erosion channel $R = 5\mathrm{mm}$. The initial dry density of buffer $\rho_{dry}(t=0) = 1600\,\mathrm{kg\,m}^{-3}$, the density of solid bentonite material $\rho_s = 2\,760\mathrm{kgm}^{-3}$, the width of the buffer is $95\mathrm{mm}$, and the length of the erosion channel $100\mathrm{mm}$. We have also assumed that the mass of a bentonite particle compared to flow velocity is negligible in Eq. (23), allowing one to set it zero. This approximation is allowed since for the volumetric flow rates in regime $Q \in \left[\frac{10^{-5}}{600}, \frac{10^{-3}}{600} \right] \frac{1}{\mathrm{min}}$, and for bentonite particles of diameter $200\mathrm{nm}$ and thickness of $1\mathrm{nm}$ (Liu 2009), the Stoke's velocity is at least three orders of magnitude smaller as the volumetric flow rate divided by channel cross sectional surface area.

Furthermore, the boundary conditions for the bentonite concentration in erosion channel are such that concentration is zero at the inlet, and normal flux extrudes through the top of the channel at any given time. Furthermore, at the rock boundary all the fluxes go to zero. The initial suction is calculated by van Genuchten expression from the initial dry density, see Eq. (5), and the initial suction at water equals to zero. The initial concentration of bentonite in the buffer was assumed to be $r_{dry}\ 0\ = 1\,600\mathrm{kgm}^{-3}$.

4. Numerical results for total eroded mass and clay particle concentration in channel

We have calculated the concentrations of bentonite particles at the erosion channel and extracted the total mass flux passing through the top of the channel

$$m_{acc}\ t\ = \int_0^t dt' \int dA c\ r, L, t'\ \ v(r.t') \equiv \int_0^t dt'\ m_{er}(t'), \quad (25)$$

presenting here the mass loss of bentonite from one cylindrical erosion channel with respect to time. The erosion rate is defined as a time derivative of the total mass flux, and is given in units of mass per second. Although namely different, this definition is in accord with the one given in (SKB 2008) concerning experimental erosion rates, which were given as eroded mass per flown volume of eroding water. Since we are using only constant volumetric flow rates, the total flown volume of eroding water is a linear function of time.

In Eq. (25) $c(r, L, t)$ is the concentration of bentonite particles in eroding liquid at the outlet of the channel. Figures 5 and 6 show how the erosion rate depends on suction induced bulk modulus κ_s and saturated hydraulic conductivity K_0. It is clearly seen, that erosion rate as well as accumulated eroded mass (Figs. 3 and 4) increase as a function of the suction induced bulk modulus κ_s and decreases as a function of the saturated hydraulic permeability K_0. Moreover, the accumulated mass m_{er} increases as a power law of simulation time up to time scale that is determined by the saturation time of erosion buffer. After the dry density saturates to the limiting critical concentration, the accumulated mass curve plateaus and does not increase any further, which is naturally set by the form of Eq. (20).

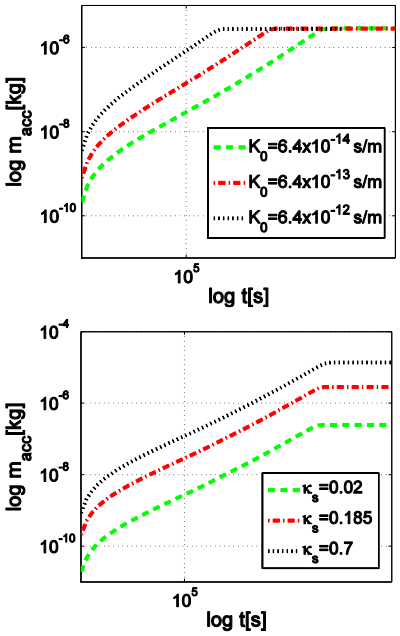

Figs. 3 and 4. Accumulated eroded mass as a function of time in double-logarithmic plot for various κ_s (Fig. 3) and K_0 (Fig. 4).

5. Conclusions and discussion

In this article we have reported about the preliminary results on modeling and experiments about the eroded mass loss from a single cylindrical erosion channel as a function of various physical parameters. The theoretical formulation developed applies for arbitrary geometry, but the numerical simulations were done under the assumptions of a constant channel radius, and such that deformation of the buffer is fully induced by the suction of groundwater into initially dry buffer material. The erosion rates and total eroded masses measured from experiments (Hanana 2010, SKB 2006, SKB 2008) are in qualitative agreement with our numerical modeling (Punkkinen 2010a).

The main conclusion of the theoretical and numerical study is that the absolute mass loss over long time mainly depends on the suction induced bulk modulus κ_s, that in the current model is assumed to cause the free swelling. We have shown in this article, that under the assumption that free swelling is induced only by suction gradient, the asymptotic dry density is determined by the suction induced bulk modulus, the initial dry density and the initial water content (suction) of dry buffer material, see Eq. (20). In addition, the rate at which the erosion happens is strongly increased as a function of the suction induced bulk modulus, and decreased as a function of the saturated hydraulic conductivity K_0.

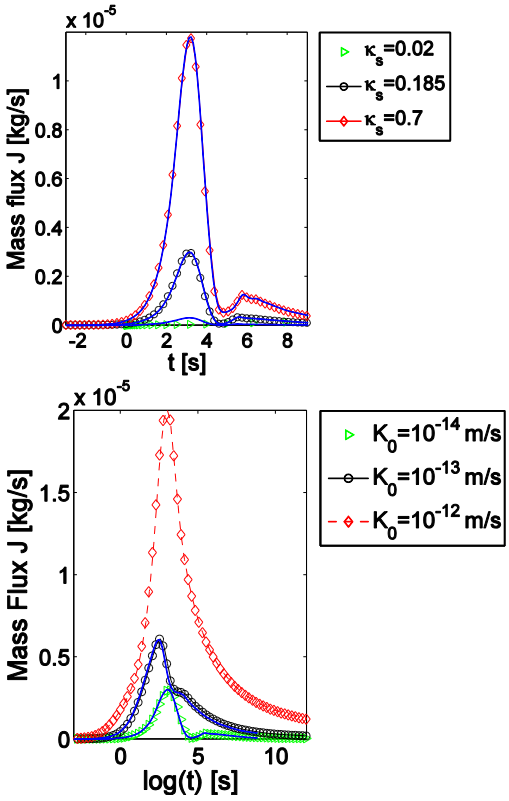

Figs. 5 and 6. Erosion rate as a function of logarithmic time for various κ_s (5) and K_0.

We have determined the time dependence of the total eroded mass, and based on our numerical results we propose that, in active regime of erosion between the initial lag time $t_0 (\approx 10^3 \text{s})$ and the saturation time of the bentonite $(\approx 4 \cdot 10^7 \text{s} \cong 14\text{y})$, it follows the scaling law

$$m_{acc}\ t\ = m_0 \left[\frac{t}{t_0} \right]^{\alpha} \equiv m_0 \left[\frac{m_w}{m_{w,0}} \right]^{\alpha}, \qquad (28)$$

where the exponent $\alpha \in 0.7,1$ depends on several different factors, such as volumetric flow rate Q, suction induced bulk modulus κ_s and the saturated hydraulic conductivity of the water K_0 penetrating into dry bentonite clay. It seems that the exponent α approaches one for small volumetric flow rate, small suction induced bulk modulus, and large hydraulic conductivity, see Figures 3, 4, 5 and 6. On the other hand, α approaches 0.7 for strong volumetric flow rate of order 100ml/min, large enough suction induced bulk modulus κ_s, and small enough saturated hydraulic conductivity K_0.

One of the main issues left open in the current work, is how the groundwater salt concentration modifies the erosion rates and accumulated mass losses. This work is in progress and we will report it by the end of 2011.

6. References

Alonso E., Gens A., & Josa A., *Géotechnique,* **40** No. 3, 405-430 (1990).

Bonelli S. & Brivois O., *Int. J. Numer. Anal. Meth. Geomech.*, **32**, 1573-1595 (2008).

Caputo J.-G., *Transp. Porous Med.,* **74**, 1-20 (2008).

Hanana K., Punkkinen O. & Autio J., Posiva Report (2010).

Schoneberg J. A. & Hinch E.J., *J. Fluid mech.*, **203**, 517-524 (1989).

Liu L., Moreno L., & I. Neretnieks, *Langmuir***, 25**, 679-687 (2009).

Punkkinen O., Koskinen K., Autio J. & Olin M., Nantes Conference Article, (2010a).

Punkkinen O., Koskinen K., Autio J., Pulkkanen V.-M. & Olin M., Pre-saturation erosion, Posiva working report (2010b).

SKB, TR-06-80 (2006).

SKB, TR-08-135 (2008).

7. Acknowledgements

This work is commissioned and supported by Posiva Oy in Finland.